13th World Conference on Earthquake Engineering
Vancouver, B.C., Canada
August 1-6, 2004
Paper No. 881

EFFECT OF P−Δ ACTION OF ACTUATORS IN A HYBRID LOADING TEST

Seiji NAGATA[1], Kazuhiko KAWASHIMA[2], Gakuho WATANABE[3]

SUMMARY

In a hybrid loading test, actuators are usually pin connected to a specimen at one end and a loading frame at the other end. Under this condition, if the structure is loaded, a secondary force is induced by actuators due to P−Δ action of actuators. This P−Δ action of actuators is important in a hybrid loading test, because ignoring this leads to a wrong test result. This paper presents a numerical simulation and a bench mark hybrid loading test to show the importance and modification of the P−Δ action in a hybrid loading test.

INTRODUCTION

To evaluate the seismic performance of a structural system or a structural component with hysteretic behavior, a hybrid loading test is often used. In a standard setup, three actuators are used to provide two lateral loads in *x* and *y* directions and a vertical load in *z* direction. The actuators are generally pin connected to the structure at one end and a loading frame at the other end. Under this condition, if the two lateral actuators push the structure in *x* and *y* directions, a lateral force component is induced in *x* and *y* directions by the lateral actuators set in *y* and *x* directions, respectively, due to P−Δ action of actuator forces. A lateral force component is also induced in *x* and *y* directions by the vertical actuator. This effect is called here as a P−Δ action of actuators. It is important to include the P−Δ action of actuators in a loading test. In particular, the P−Δ action of actuators is important in a hybrid loading test, because ignoring this effect may lead to a wrong test result.

A hybrid loading test on a single cantilevered column taking account of the P−Δ action of actuators is clarified based on a numerical simulation and a bench mark test in this paper.

[1] Graduate Student, Tokyo Institute of Technology, Tokyo, Japan. Email: nseiji@cv.titech.ac.jp
[2] Professor, Tokyo Institute of Technology, Tokyo, Japan. Email: kawasima@cv.titech.ac.jp
[3] Research Associate, Tokyo Institute of Technology, Tokyo, Japan. Email: gappo@cv.titech.ac.jp

P–Δ ACTION OF ACTUATORS AND ITS MODIFICATION

When we idealize a cantilevered column as a three-degree-of-freedom system using three actuators (two horizontal and one vertical) as shown in Fig. 1, the equations of motion of the column are

$$[M]\{\ddot{u}_{t+\Delta t}\}+[C]\{\dot{u}_{t+\Delta t}\}+\{R_{t+\Delta t}\}-\{P_{GP\,t+\Delta t}\}=\{F_{t+\Delta t}\} \tag{1}$$

in which $[M]$ and $[C]$: mass and damping matrices, respectively, $\{\ddot{u}_{t+\Delta t}\}$ and $\{\dot{u}_{t+\Delta t}\}$: accelerations and velocities, respectively, $\{R_{t+\Delta t}\}$: restoring forces of the specimen, $\{P_{GPt+\Delta t}\}$: forces induced by the geometrical P–Δ effect and $\{R_{t+\Delta t}\}$: external forces. The subscript represents the time dependent quantities at time $t + \Delta t$. In the following, the subscript $t + \Delta t$ is deleted for simplicity.

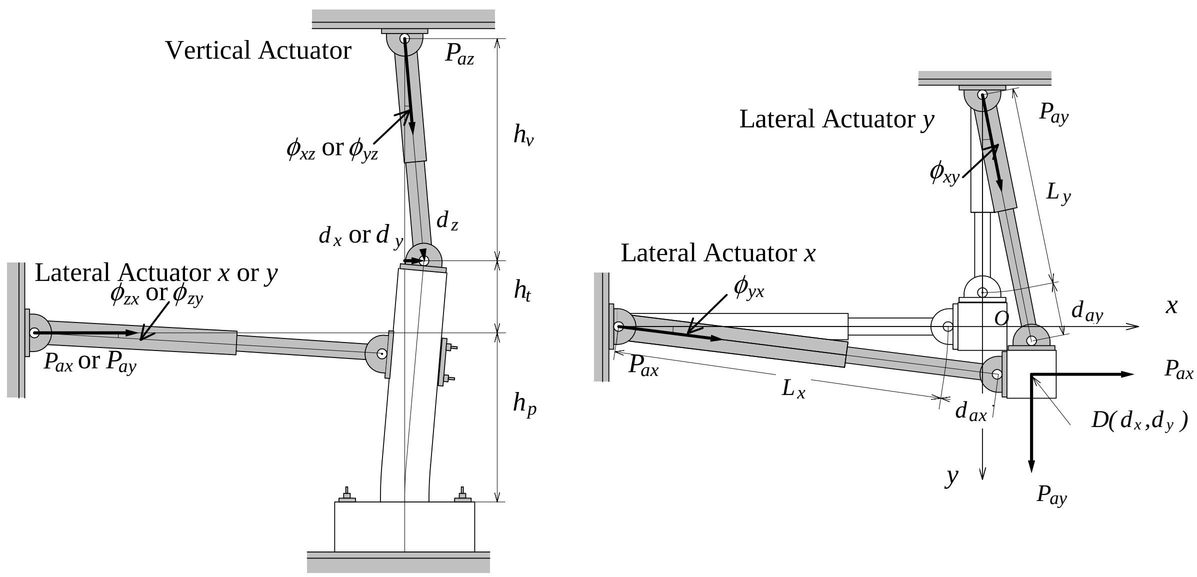

(a) Side View (b) Plane View

Fig. 1 P–Δ Action by Actuators (Setup I)

If three actuators are pin connected by swivels to a specimen and a loading frame at both ends as shown in Fig. 1 (setup I), the lateral forces which are applied to the specimen by the actuators, $\{P_a\}=\{P_{ax}, P_{ay}, P_{az}\}^T$, are

$$\{P_a\}=[T]^{-1}\{\{R\}-\{P_{GP}\}\} \tag{2}$$

where

$$\{R\}=\begin{Bmatrix} R_x \\ R_y \\ R_z \end{Bmatrix} \tag{3}$$

$$[T]=\begin{bmatrix} \cos\phi_{yx} & \sin\phi_{xy} & (1+h_t/h_p)\sin\phi_{xz} \\ \sin\phi_{xy} & \cos\phi_{yx} & (1+h_t/h_p)\sin\phi_{yz} \\ \sin\phi_{zx} & \sin\phi_{zy} & \cos\phi_{zx}\cos\phi_{zy} \end{bmatrix} \tag{4}$$

$$\{P_{GP}\} = \begin{Bmatrix} P_{GPx} \\ P_{GPy} \\ P_{GPz} \end{Bmatrix} = \frac{P_{az}}{h_p} \begin{Bmatrix} d_x \\ d_y \\ 0 \end{Bmatrix} \tag{5}$$

in which, $\{R\}$: restoring forces of the specimen, $\{P_{GP}\}$: forces induced by the geometrical P–Δ effect, $\{P_{AP}\}$: forces induced by the P–Δ action of actuators, ϕ_{yx} and ϕ_{xy} : angles of rotation of actuators *x* and *y*, respectively, in *x*-*y* plane, ϕ_{xz} and ϕ_{yz} : angles of rotation of vertical actuator (*z*) in *x*-*z* and *y*-*z* planes, respectively, ϕ_{zx} and ϕ_{zy} : angles of rotation of actuator *x* in *x*-*z* plane and actuator *y* in *y*-*z* plane, respectively, d_x , d_y and d_z : displacement of the specimen at the pin of swivel of vertical actuator in *x*, *y* and *z* directions, respectively, h_p : effective column height from the bottom to the loading point of the lateral actuator, and h_t : distance between the pin of swivel of vertical actuator and the pin of swivel of the horizontal actuator, respectively. Generally, $\{P_a\}$ are measured by load cells equipped in actuators.

The vertical displacement d_z is generally much smaller than d_x or d_y because of the high stiffness of a column in the axial direction. Therefore, by assuming ϕ_{zx} and ϕ_{zy} are nearly zero, Eq. (4) can be simplified as

$$[T] = \begin{bmatrix} \cos\phi_{yx} & \sin\phi_{xy} & (1 + h_t / h_p)\sin\phi_{xz} \\ \sin\phi_{xy} & \cos\phi_{yx} & (1 + h_t / h_p)\sin\phi_{yz} \\ 0 & 0 & 1 \end{bmatrix} \tag{6}$$

Consequently, the forces which compensate the P–Δ action of actuators have to be used in solving Eq. (1) as

$$[M]\{\ddot{u}_{t+\Delta t}\} + [C]\{\dot{u}_{t+\Delta t}\} + \{P_m\} = \{F_{t+\Delta t}\} \tag{7}$$

where

$$\{P_m\} = \{R\} - \{P_{GP}\} = [T]\{P_a\} \tag{8}$$

Therefore, it is important to note here that if we use the forces measured by load cells equipped in actuators $\{P_a\}$ in solving Eq. (7), an error is developed in computing the response of a structure at next time step.

It is noted that if we use a load setup in which actuators can slide keeping their original axes so that they follow the displacement of a specimen as shown in Fig. 2 (setup II), the rotations of actuators are zero in Eq. (6). If we set actuators to the specimen so that h_t =0, the P–Δ action of actuators does not exist. Consequently, Eq. (8) becomes

$$\{P_m\} = \{P_a\} \tag{9}$$

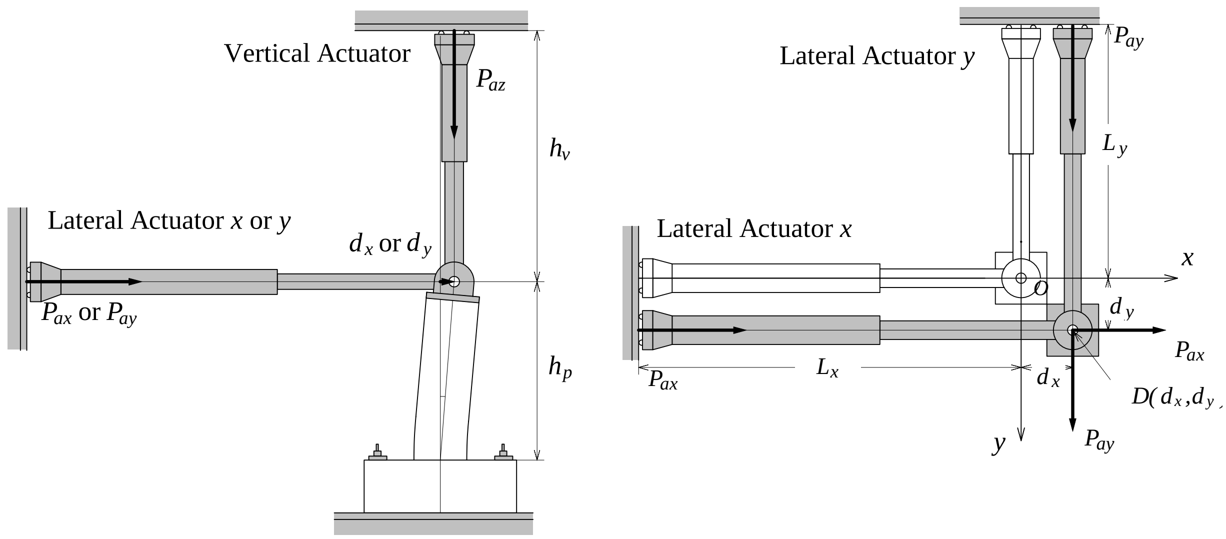

(a) Side View (b) Plane View

Fig. 2 Setup of Actuators which does not Result in P–Δ Action by Actuators (Setup II)

NUMERICAL SIMURATIONS

Model and Parameters

To clarify the effect of the P–Δ action of actuators on a hybrid loading test, a numerical simulation was first conducted using a MTS hybrid loading simulation system (Test-Star TM4.0B Program for Pseudodynamic Testing). This system was provided by MTS to conduct a simulation on the seismic response for a given condition. A time-step numerical integration scheme which avoids displacement overshooting using a displacement reduction factor is employed in the simulation system [1]. One of the features of this scheme is to have an iteration process based on the initial stiffness of a structure. This is because of avoiding undesirable loading and unloading hysteresis during iterations.

In the simulation, a 1.35 m tall (effective height) reinforced concrete column with a 0.4 m x 0.4 m rectangular section was analyzed. The restoring forces were idealized by an elasto-plastic with the identical stiffness and yield strength in both x and y directions. Since the axial stiffness of the column is very high, Eq. (7) was solved by eliminating the vertical response. A constant vertical force of 160 kN was assumed in the simulation.

A numerical analysis was conducted assuming the setup I under two cases; unilateral and bilateral excitations under a constant vertical load. In both cases, Eq. (7) was solved using Eq. (8) or Eq. (9). It is obvious that an error may be developed if we use Eq. (9) under the setup I. It is the purpose of this numerical simulation to clarify whether we can have an approximate solution which is virtually identical to the exact solution if we use Eq. (8) in the setup I. The solution solved by Eqs. (7) and (9) under the setup II was regarded as the exact solution.

A ground acceleration recorded at JMA Kobe Observatory during the 1995 Kobe earthquake was used as an input motion by scaling down its intensity to 30 % of the original. NS and EW components were used in the x and y directions, respectively. Damping ratios were assumed as 5 %. Time increment was 0.01 second.

Effect of P−Δ Action of Actuators

If we use the setup II, the lateral force vs. lateral displacement hysteresis of the column at the loading point becomes as shown in Fig. 3 (2). There exists no P−Δ action of actuators in this setup. It is noted that since the geometrical P−Δ effect is included in the lateral forces measured by the lateral actuators, P_{ax} and P_{ay}, the post-yield stiffness is slightly negative. On the other hand, Fig. 3 (1) shows the hysteresis of the column under the setup I. The lateral forces measured by the lateral actuators, P_{ax} and P_{ay}, have a larger negative stiffness at the post-yield range. If we use P_{ax} and P_{ay} in solving Eq. (7), we must have an error due to the P−Δ action of actuators as described above. Therefore, P_{mx} and P_{my} by Eq. (8) have to be evaluated in solving Eq. (7) to eliminate the P−Δ action of actuators.

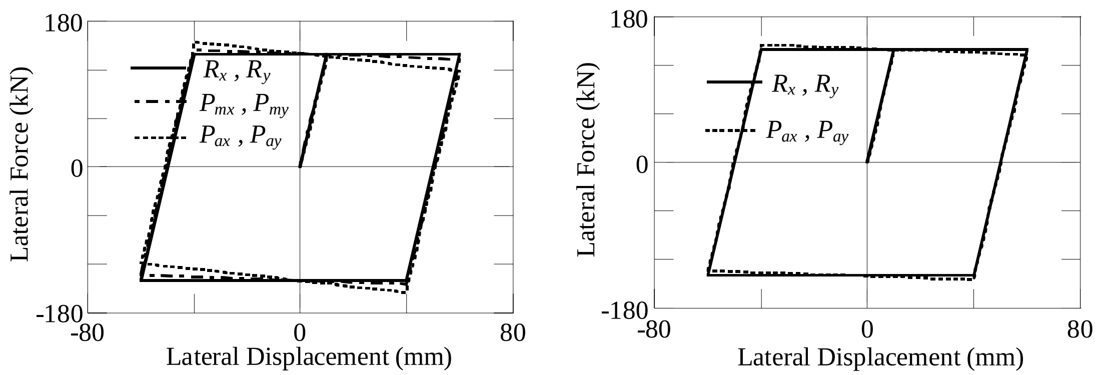

(1) Setup I (2) Setup II

Fig. 3 Lateral Force vs. Lateral Displacement Hystereses for the Numerical Simulations

Fig. 4 shows the computed response displacements of the column subjected to the unilateral excitation under the constant vertical load. They were computed under three conditions; (1) setup II, (2) setup I without modification on the P−Δ action of actuators, and (3) setup I with modification on the P−Δ action of actuators by Eq. (8). It is noted here that the response displacement computed under the setup II is the exact solution. The column displacement starts to increase at 5 s, and a large biased response occurs at

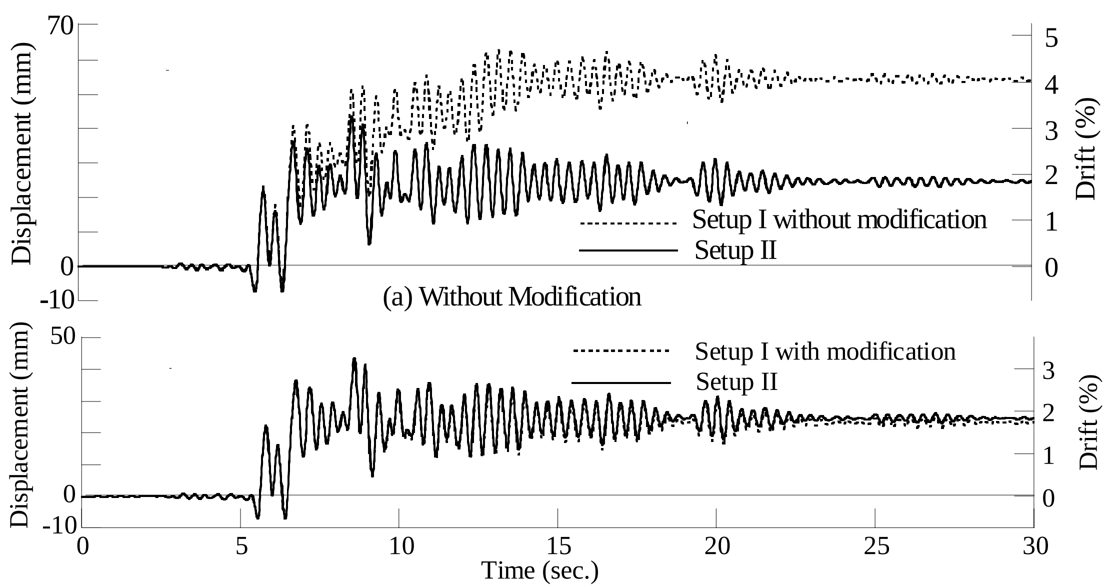

(b) With Modification

Fig. 4 Effect of P−Δ Action of Actuators under the Unilateral Excitation about 7 s in the exact solution. As a consequence, a residual drift of 1.8 % remains at the end of the excitation. On the other hand, if we use the setup I without modification on the P–Δ action of actuators, the response displacement is much larger than the exact solution, and the residual drift reaches 4%. However, the column displacement becomes virtually the same with the exact solution by providing the modification on the effect of P–Δ action of actuators.

Fig. 5 shows the same comparison for the column subjected to the bilateral excitation under the constant vertical load. Exactly the same results are obtained under the bilateral excitation as well.

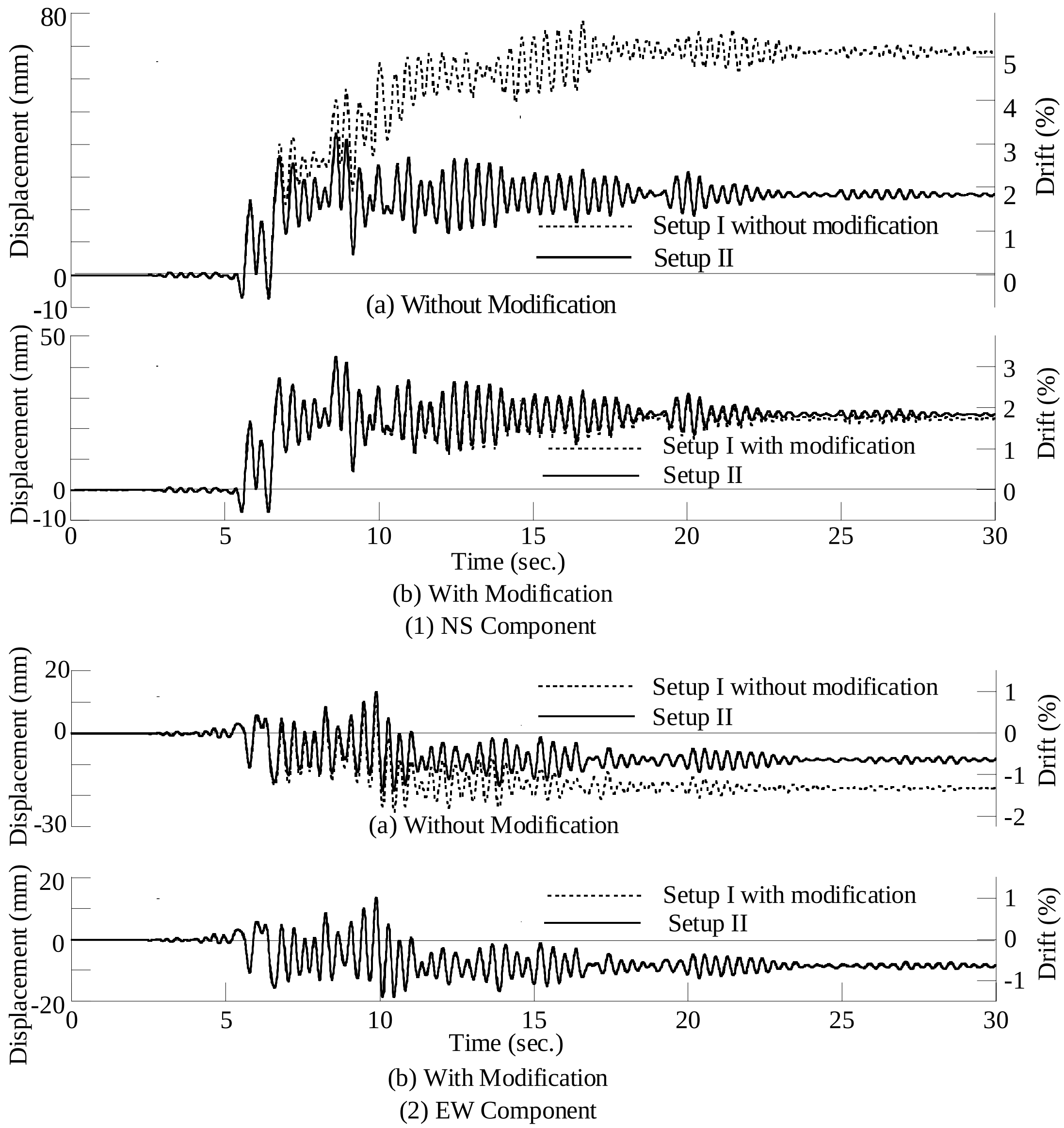

Fig. 5 Effect of P–Δ Action of Actuators under the Bilateral Excitation

AN EXPERIMENTAL CLARIFICATION

Test Specimens and Parameters

Application of the above simulation was clarified based on a hybrid loading test on two single cantilevered columns as shown in Fig. 6. Because the stiffness property can be assessed from the section quantities, a H-shape beam with 176 mm width and 200 mm height was used as a model column. The effectiveness of the modification on P–Δ action of actuators may be verified by correlating the test results by the fiber element analysis. If the hybrid loading test provides a response close to the one by the fiber element analysis, the effectiveness of the modification can be assured. For such a purpose, it was important to use the specimens with known stiffness and section properties. The H-shape beam was anchored into a reinforced concrete footing to set to a test floor. The yield strength of the H-shape beam was 249 MPa (JIS SS400). The footing was enough reinforced so that damage did not occur in the footing.

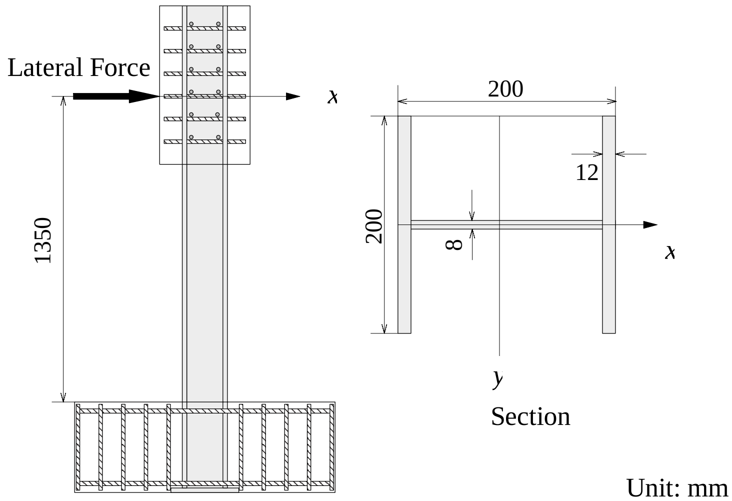

Fig. 6 Test Model

One of the two columns was loaded in the unilateral direction (strong axis) and the other was loaded bilateral direction under a constant vertical load of 100 kN. The JMA Kobe ground acceleration was used as an input motion by scaling down the intensity to 10 % and 30 % of the original. NS component was used in the *x* direction under the unilateral excitation, and NS and EW components were used in the *x* and *y* directions, respectively, under the bilateral excitation. The specimens were first loaded by the JMA Kobe ground acceleration with 10 % intensity of the original, and then loaded by the same ground acceleration with 30% intensity. Since the specimens slightly suffered damage by the 10 % intensity excitation, as will be described later, the accumulation of damage occurred during the excitation by 30 % intensity ground acceleration. This makes the analytical correlation by the fiber element method difficult on the second run.

The masses which were lumped at the top of the specimen were assumed as 30 t and 12 t in the *x* and *y* directions, respectively. Damping ratios were assumed as 5 % for the first and second modes. Initial stiffness was assumed as 6.0 kN/mm and 2.5 kN/mm in *x* and *y* directions, respectively, based on a cyclic loading test with a displacement amplitude of 2 mm which conducted before the hybrid loading test. Since the natural period of the specimen with the above masses is 0.444 s and 0.436 s in the *x* and *y* directions, it was assumed as 0.44 s in both *x* and *y* directions, respectively in the simulation.

Seismic Response of the Bench Mark Models

Fig. 7 shows the response displacements of the model subjected to the 10 % of JMA Kobe ground acceleration. Responses under both the unilateral and bilateral excitations are presented here. The maximum displacement was 0.7 % drift under the unilateral excitation, while it was 0.7 % and 0.3 % drift in *x* and *y* directions, respectively, under the bilateral excitation. Residual drifts were not significant in both tests. The H-shape steel and the footing did not suffer visible damage in both tests.

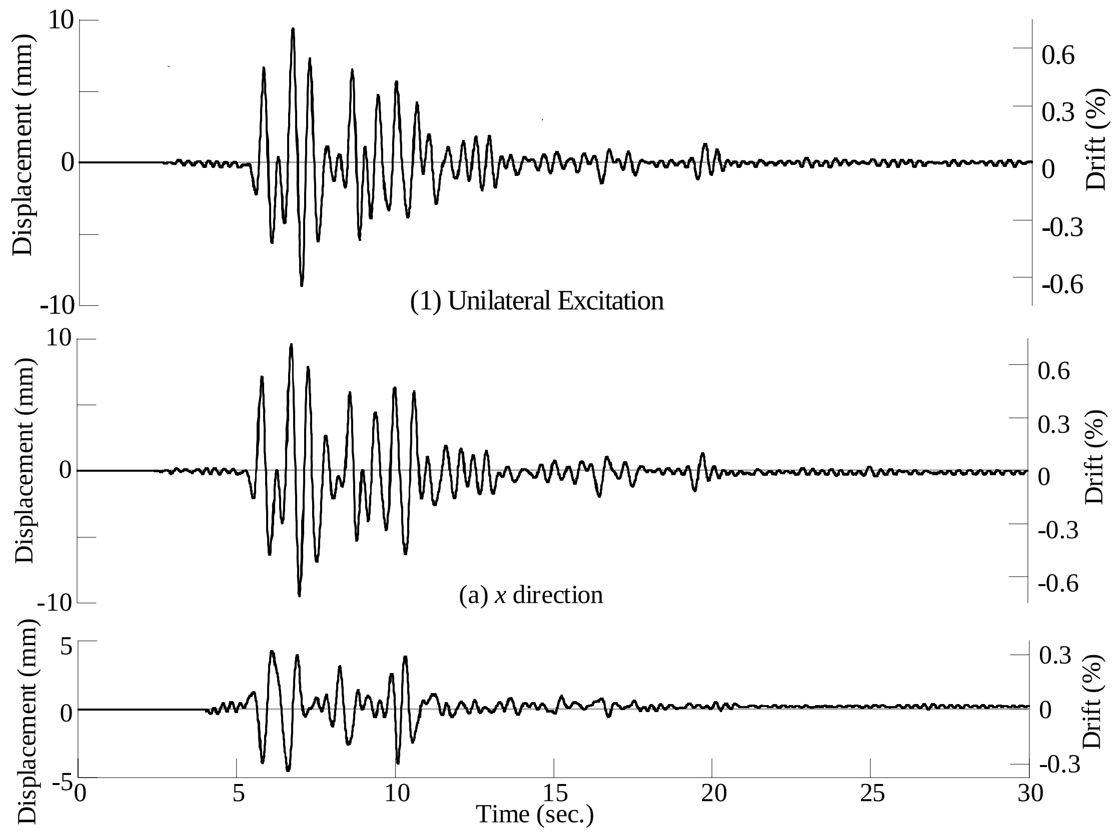

(b) y direction

(2) Bilateral Excitation

Fig. 7 Seismic Response Displacement under 10 % JMA Kobe Excitation

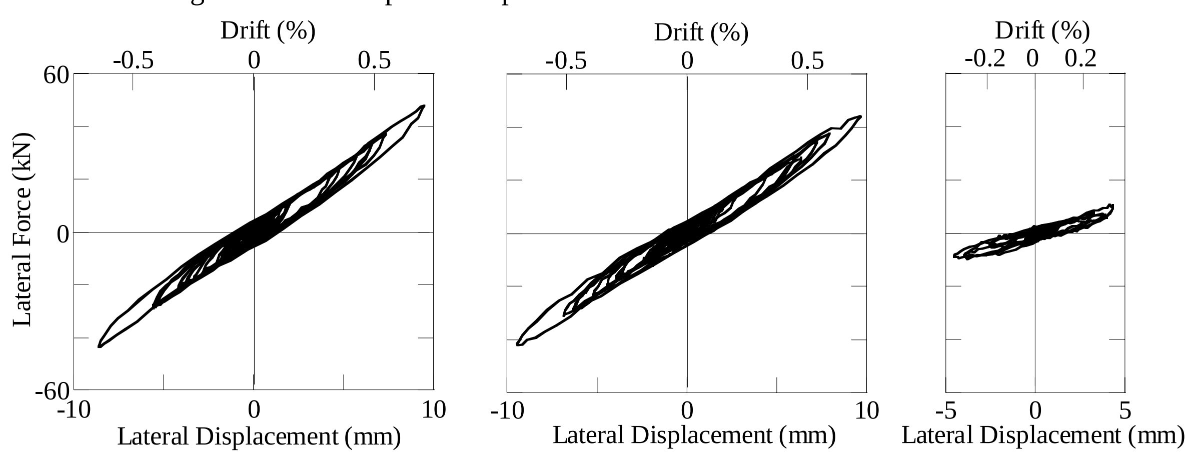

(a) x direction (b) y direction

(1) Unilateral Excitation (2) Bilateral Excitation

Fig. 8 Lateral Force vs. Lateral Displacement Hystereses of Specimen under 10 % JMA Kobe Excitation

Fig. 8 shows the lateral force vs. lateral displacement hystereses at the loading point. The maximum restoring force was 47 kN under the unilateral excitation, and 44 kN and 10 kN in the x and y directions, respectively, under the bilateral excitation. Because the nominal yield strength of the H-shape beam is about 85 kN and 30 kN in the x and y directions, respectively, H-shape beam did not yield during the 10 %

JMA Kobe excitation. Slight hysteretic behavior of the lateral force vs. lateral displacement relation may be developed by the plastic deformation of the reinforced concrete around the H-shape beam in the footing.

The specimens were then loaded using 30 % of the JMA Kobe ground acceleration. Figs. 9 and 10 show the response displacements and the lateral force vs. lateral displacement hystereses. The maximum displacement was 2.4 % drift under the unilateral excitation. A residual drift of 2.4 % occurred at 11 s. On the other hand, the maximum displacement was 3.3 % and 1.9 % drift in *x* and *y* direction, respectively, under the bilateral excitation. Residual drifts of 0.7 % and 0.2 % occurred in *x* and *y* direction, respectively, at 12 s. Although the initial yield was approximately 85 kN and 30 kN in the *x* and *y* directions, the restoring forces still increased after the initial yield, and reached 110 kN under the unilateral excitation, and 104 kN and 38 kN in *x* and *y* direction, respectively, under the bilateral excitation. Extensive buckling or spalling of concrete was not observed.

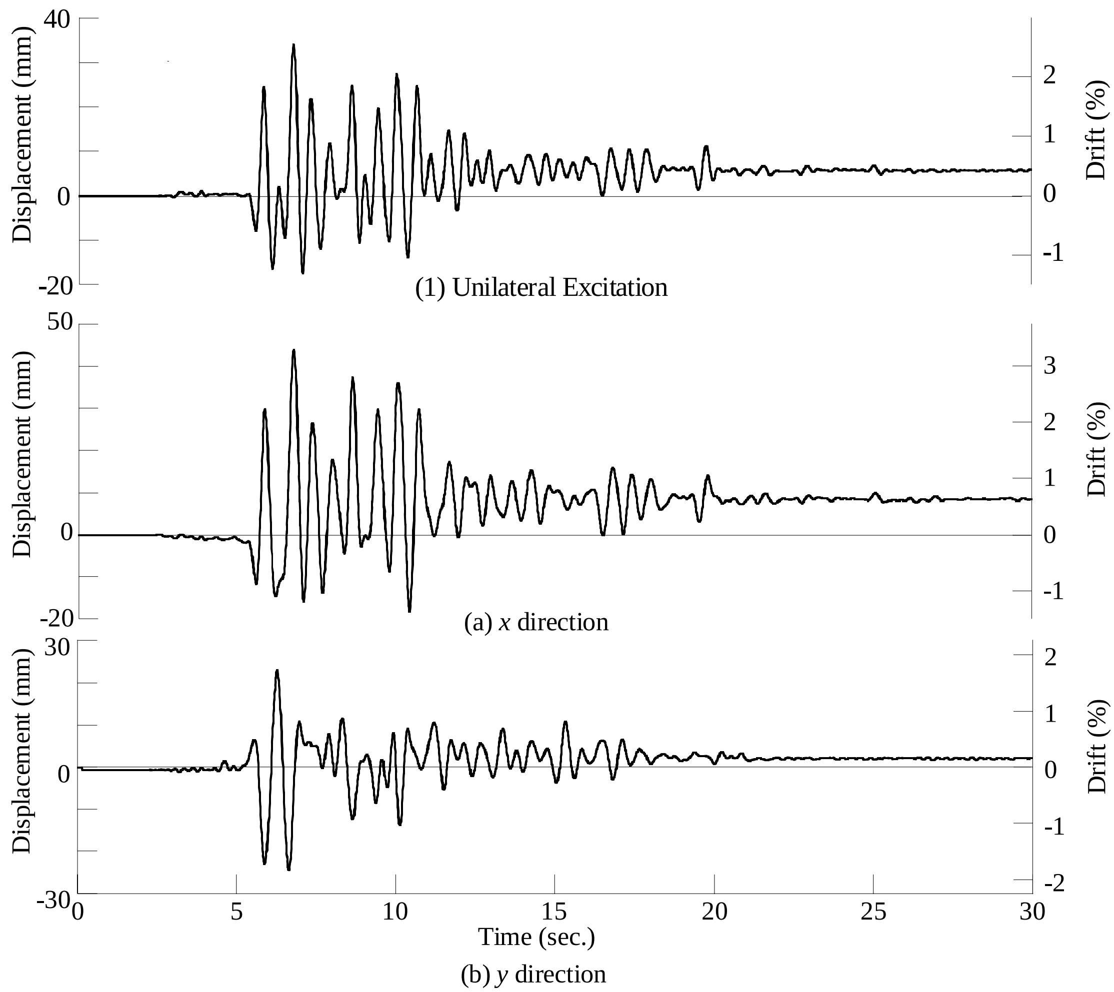

Fig. 9 Seismic Response Displacement under 30% JMA Kobe Excitation

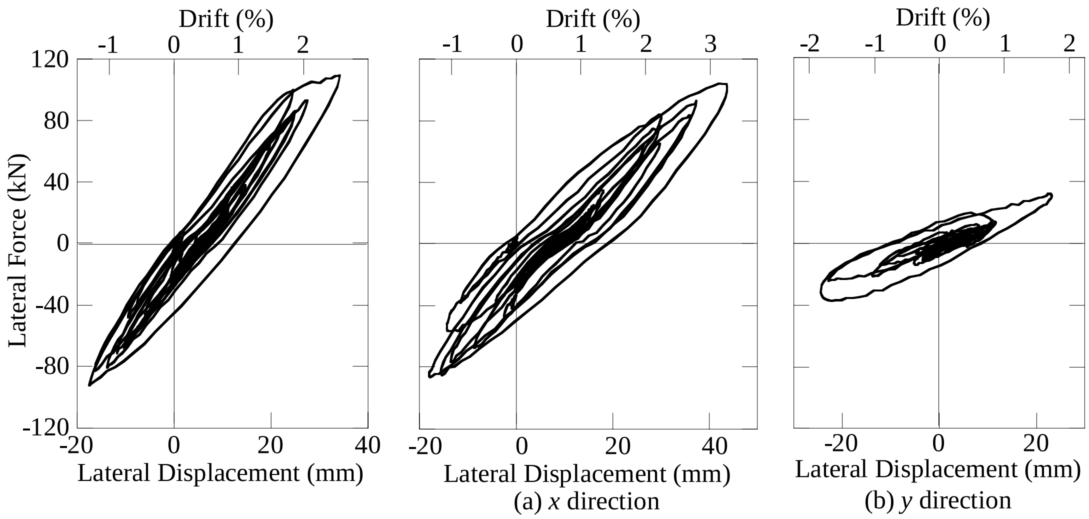

Fig. 10 Lateral Force vs. Lateral Displacement Hystereses of Specimens under 30% JMA Kobe Excitation

A FIBER ELEMENT ANALYSIS

Model and Parameters

To correlate the responses by the hybrid loading test, the specimens were idealized as shown in Fig. 11 using a fiber element at the plastic hinge. The length of plastic hinge was assumed as 150 mm. The Menegotto-Pinto model [2, 3] was used to idealize the stress vs. strain relation of the H-shape beam. As described above, since slight hysteretic behavior was observed under the 10 % JMA Kobe excitation even if the H-shape beam was still in elastic, this hysteretic behavior was idealized by providing a rotational spring at the bottom of the H-shape beam as shown in Fig. 11. Assuming a bilinear hysteresis model for the rotational spring, the initial elastic stiffness, post yield stiffness and the yield rotation were so determined that the computed lateral force vs. lateral displacement hystereses are close to the experimental results as shown in Fig. 12.

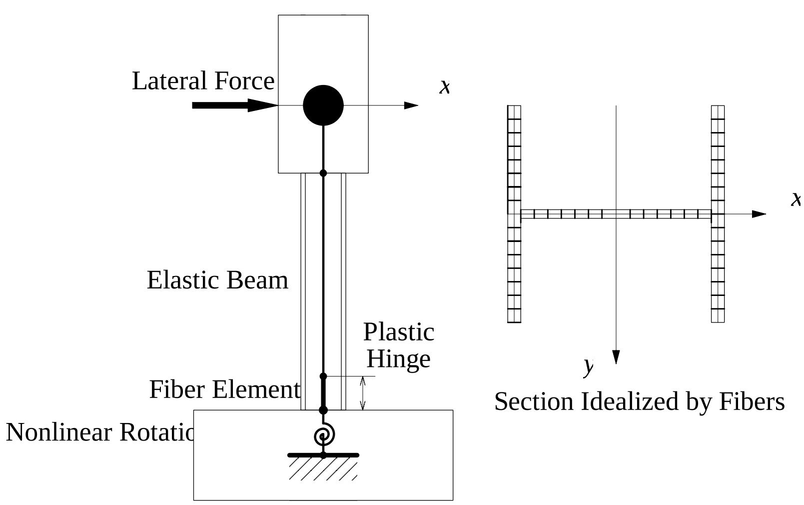

Fig. 11 Fiber Element Model

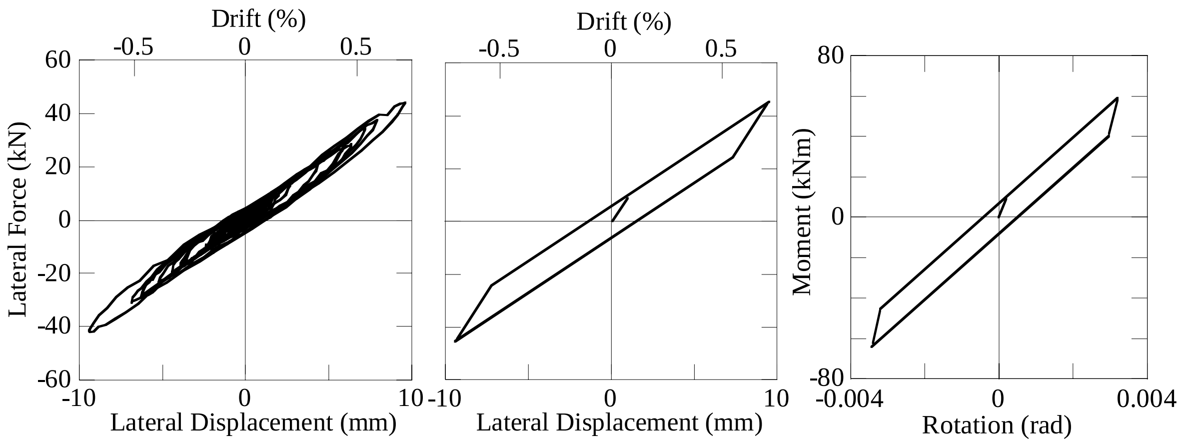

(a) Hysteresis under 10 % JMA Kobe Excitation

(b) Idealized Hysteresis in the Analysis

(c) Idealized Hysteresis of the Rotational Spring

(1) *x* direction

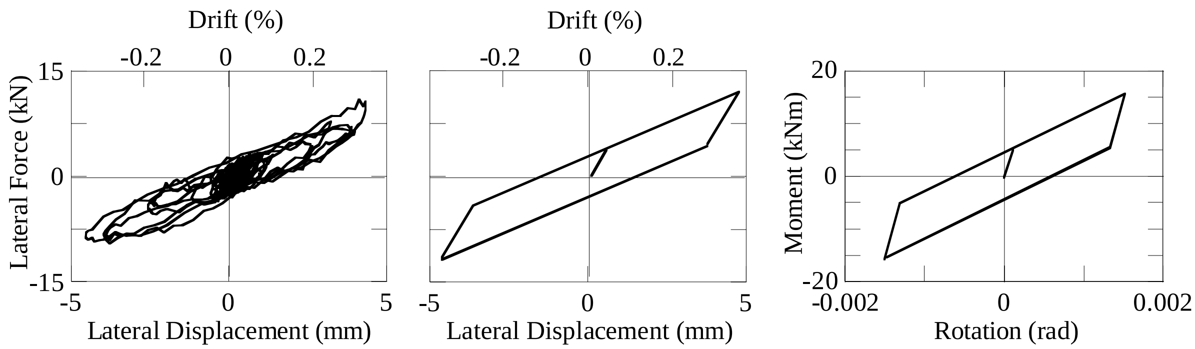

(a) Hysteresis under 10 % JMA Kobe Excitation

(b) Idealized Hysteresis in the Analysis

(c) Idealized Hysteresis of the Rotational Spring

(2) *y* direction

Fig. 12 Modeling of the Rotational Spring

Comparison of Responses between the Test and the Fiber Element Analysis

Figs. 13 and 14 compare the computed column displacement and lateral force vs. lateral displacement hystereses to the experimental results under the 10 % JMA Kobe excitation. Both the responses under the unilateral and bilateral excitations are shown here. The column displacement and the lateral force vs. lateral displacement hystereses are well correlated with the analysis under both the unilateral and the bilateral excitations. Figs. 15 and 16 show computed moment vs. curvature hystereses at the plastic hinge and moment vs. rotation hystereses at the rotational spring, respectively. The H-shape column still remains in elastic range and the hystereses at the rotational spring contributes to the hystereses of the lateral force vs. lateral displacement relation as shown in Fig. 14. It is apparent that the responses by the hybrid loading test using Eqs. (7) and (8) provides responses which are very close to the responses predicted by the fiber element analysis. This verifies the application of Eq. (8) to compensate the P–Δ action of actuators presented herein.

The same analytical model was used to correlate the response under the 30 % JMA Kobe excitation. Because this was the second run for the same model, there must have had an accumulation of damage in the reinforced concrete of footing, which might result in a degradation of the rotational spring set at the bottom of the H-shape beam. However the same analytical model correlates the experimental responses

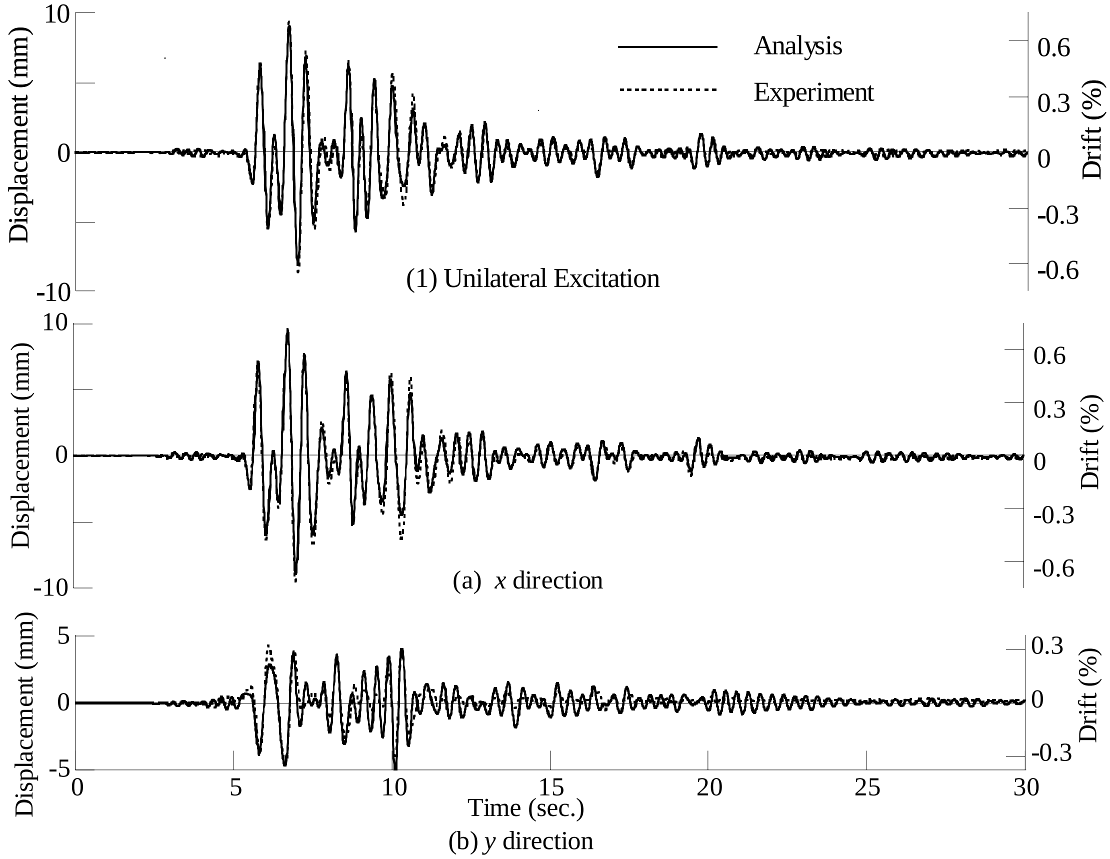

(2) Bilateral Excitation

Fig. 13 Correlation of Seismic Response Displacement by Fiber Element Analysis (10 % JMA Kobe Excitation)

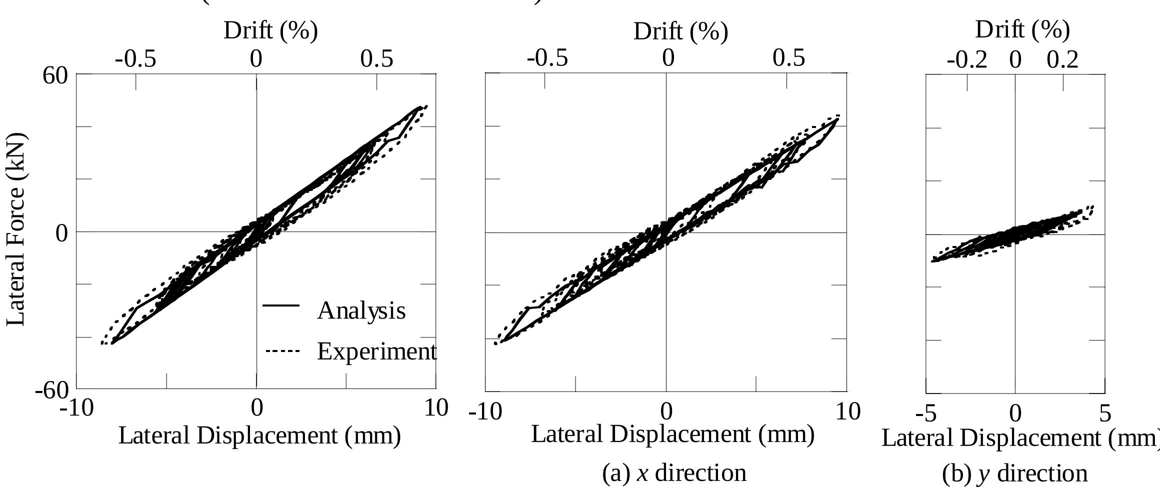

(1) Unilateral Excitation (2) Bilateral Excitation

Fig. 14 Correlation of Lateral Force vs. Lateral Displacement Hystereses (10 % JMA Kobe Excitation)

with a fairly good accuracy as shown in Figs. 17 and 18. Figs. 19 and 20 show computed moment vs. curvature hystereses at the plastic hinge and moment vs. rotation hystereses at the rotational spring, respectively. The H-shape beam shows hysteretic behavior with a peak curvature of 0.076 /m under the

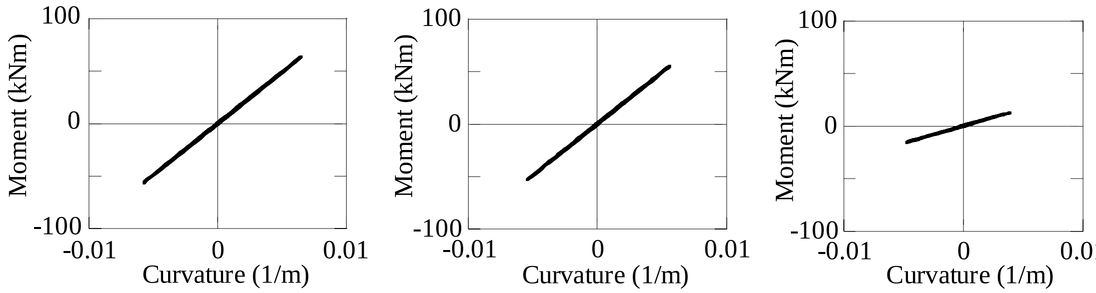

(a) *x* direction (2) *y* direction

(1) Unilateral Excitation (2) Bilateral Excitation

Fig. 15 Computed Moment vs. Curvature Hystereses at the Plastic Hinge
(10 % JMA Kobe Excitation)

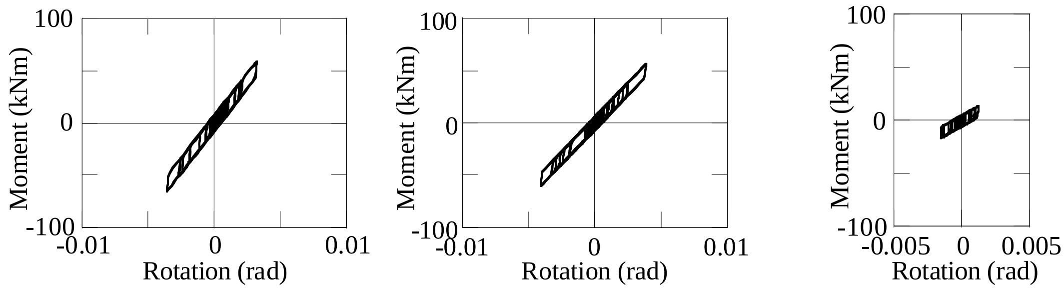

(a) *x* direction (2) *y* direction

(1) Unilateral Excitation (2) Bilateral Excitation

Fig. 16 Computed Moment vs. Rotation Hystereses at the Rotational Spring
(10 % JMA Kobe Excitation)

unilateral excitation and 0.079 /m and 0.068 /m in the *x* and *y* directions, respectively, under the bilateral excitation. The hysteretic behavior at the rotational spring is much larger than that under the 10 % JMA Kobe excitation. They contributed to the hystereses of the lateral force vs. lateral displacement relation as shown in Fig. 18.

CONCLUSIONS

This paper presents a compensation of the effect of P−Δ action of actuators in a hybrid loading test. A numerical simulation and an experimental verification were conducted to clarify the modification of the effect of P−Δ action of actuators. Based on the results presented herein, the following conclusions may be deduced:

1. The P−Δ action of actuators is important in a hybrid loading test. It has to be properly included in solving the equations of motion. Eq. (8) has to be used in the evaluation of seismic responses in a hybrid loading test.
2. If the P−Δ action of actuators is disregarded in a hybrid loading test, a larger residual drift is likely developed.
3. The hybrid loading test on two bench mark column models provide the response displacements which are quite close to the responses predicted by the fiber element analysis. This verifies the application of the modification by Eq. (8) to a hybrid loading test.

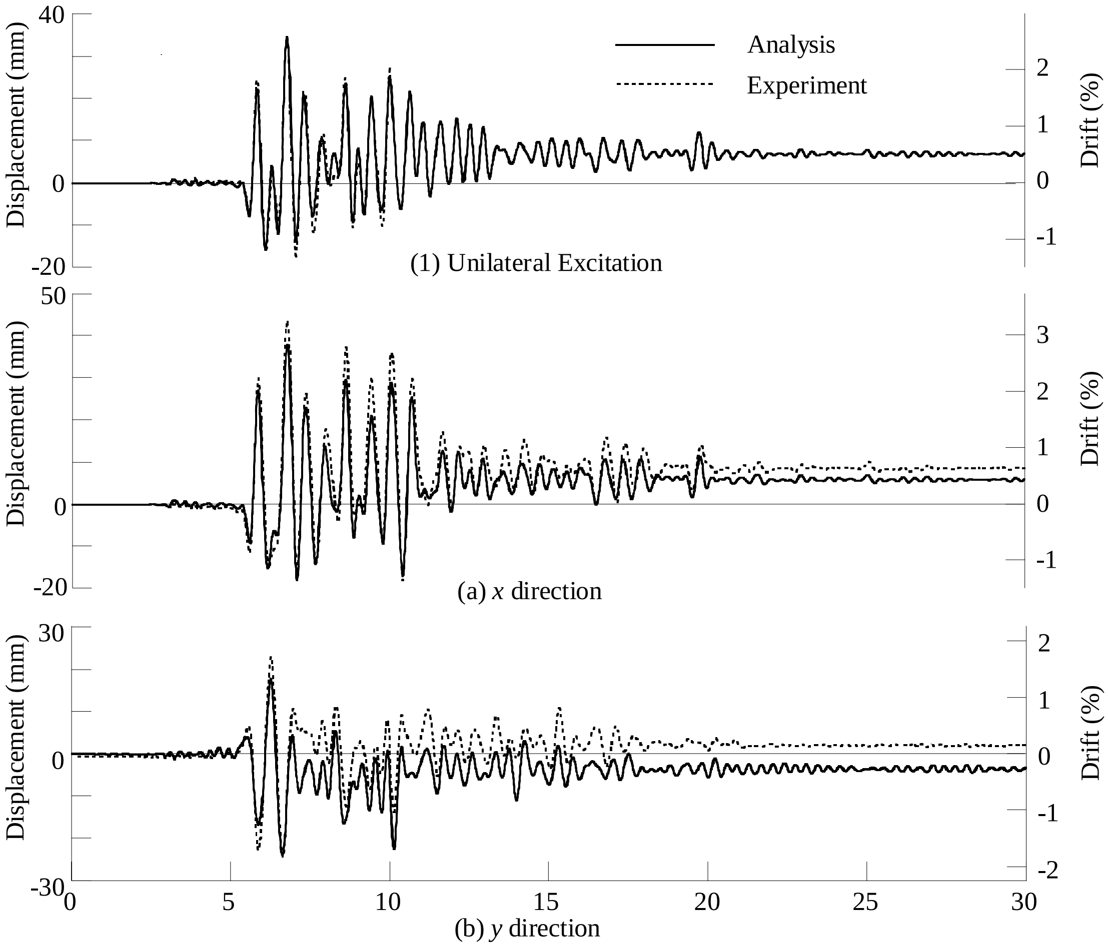

(1) Bilateral Excitation

Fig. 17 Correlation of Seismic Response Displacement by Fiber Element Analysis
(30 % JMA Kobe Excitation)

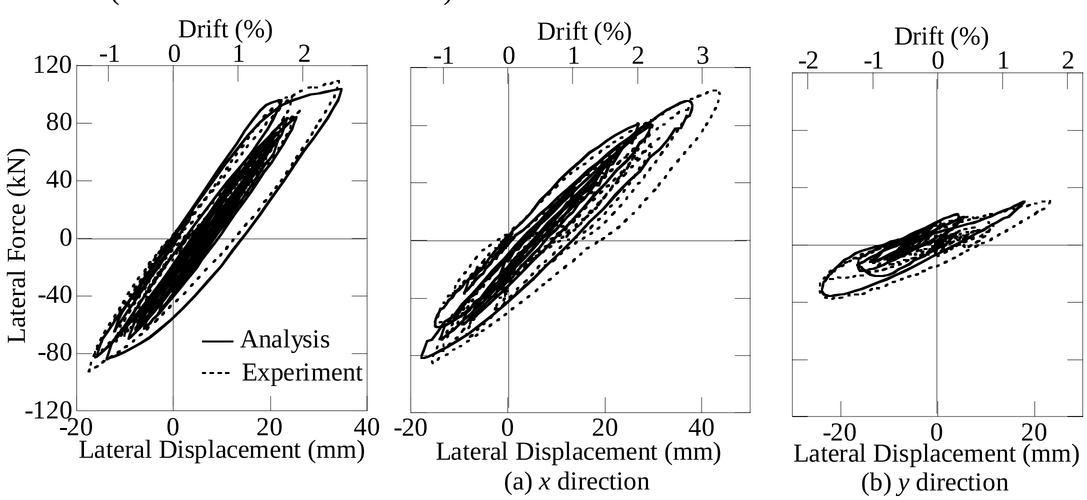

(1) Unilateral Excitation (2) Bilateral Excitation

Fig. 18 Correlation of Lateral Force vs. Lateral Displacement Hystereses
(30 % JMA Kobe Excitation)

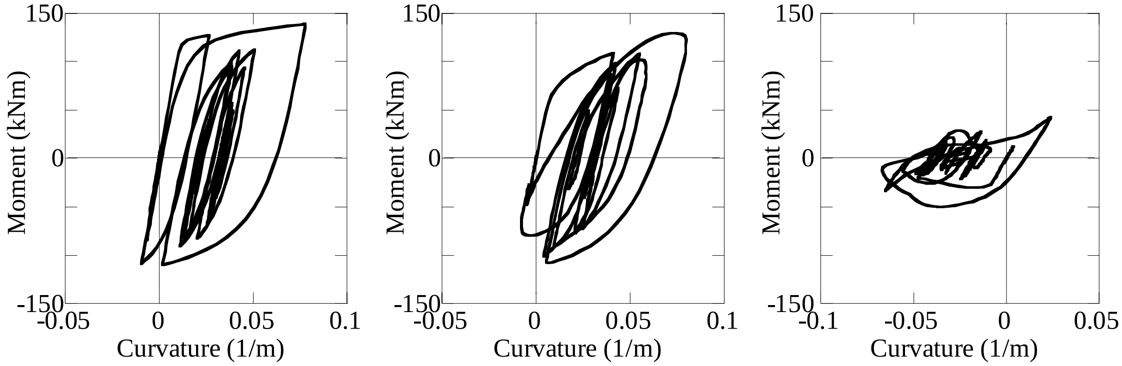

(a) *x* direction (2) *y* direction

(1) Unilateral Excitation (2) Bilateral Excitation

Fig. 19 Computed Moment vs. Curvature Hystereses at the Plastic Hinge
(30 % JMA Kobe Excitation)

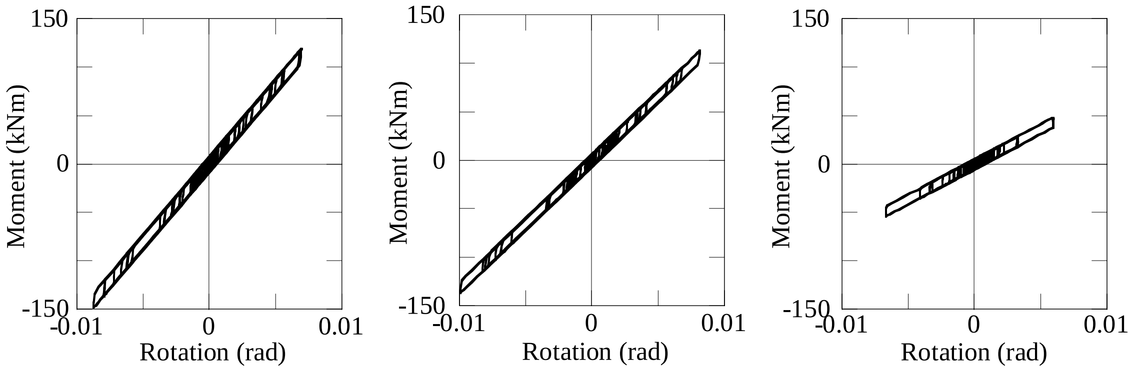

(1) Unilateral Excitation (2) Bilateral Excitation

Fig. 20 Computed Moment vs. Rotation Hystereses at the Rotational Spring
(30 % JMA Kobe Excitation)

ACKNOWLEDGEMENT

The authors express their sincere appreciation to Messrs. Nakamura, G., Hayakawa, R., Fukuda, T., Miyaji, K., Ichikawa, Y., Ogimoto, H., and Kijima, K., Department of Civil Engineering, Tokyo Institute of Technology, for kind cooperation of constriction of models and the execution of hybrid loading test.

REFFERNCES

1. Shing, P, B., Vannan, M.T. and Cater, E.(1991), "Implicit Time Integration for Pseudodynamic Tests." *Earthquake Engng. Struct. Dyn*, Vol. 20, 551-576.
2. Menegotto, M. and Pinto, P.E.(1973), "Method of Analysis for Cyclically Loaded R.C. Plane Frames including Changes in Geometry and Non-Elastic Behavior of Elements under Combined Normal Force and Bending." *Proc. of IABSE Symposium on Resistance and Ultimate Deformability of Structures Acted on by Well Defined Repeated Loads*, 15-22.
3. Sakai, J., and Kawashima, K. (2003), "Modification of the Giuffre, Menegotto and Pint Model for Unloading and Reloading Paths with Small Strain Variations." *J. Structural Mechanics and Earthquake Engineering*, JSCE, No. 738/I-64, 159-169.